

# Estimation of stresses in atmospheric ice during galloping of power transmission lines

Majid Kermani, Masoud Farzaneh and László E. Kollár

NSERC/Hydro-Québec/UQAC Industrial Chair on Atmospheric Icing of Power Network Equipment (CIGELE), and Canada Research Chair on Atmospheric Icing Engineering of Power Networks (INGIVRE), Université du Québec à Chicoutimi, Chicoutimi, Qué., Canada G7H 2B1 (www.cigele.ca)

**Abstract--**Galloping is a well-known phenomenon which occurs when wind acts on asymmetrically iced overhead cables. The resulting high amplitude vibration creates stresses in the cable and consequently in the ice covering the cable, which may result in ice failure and eventually ice shedding. The purpose of this paper is to estimate these stresses. To achieve this goal, galloping was simulated on an ice-covered cable by appropriate modification of existing models for bare cables submitted to galloping. The results of this simulation served as inputs for a new model developed by using ABAQUS, a commercial finite element software, in order to simulate the loading conditions of a chunk of atmospheric ice in the middle of a span. The positions of both ends of the ice chunk during one cycle of galloping were set as boundary conditions in this model. Results show that the elements of atmospheric ice at the top and bottom of the cable endure maximum stress.

## I. INTRODUCTION

After many years of improvements in the design of power transmission lines, they are still vulnerable to winds and storms, particularly in cold regions where atmospheric ice accretes on network equipment. The three types of vibrations created by wind on power transmission lines are galloping, aeolian vibration and wake-induced oscillation. These vibrations are associated with bending and additional tension in the cables, which can lead to damage to the power network. If ice accumulates on the cable, then stresses will develop in the ice which may lead to ice shedding; the physical phenomenon that occurs when the ice coating a cable suddenly drops off, either naturally or by means of some form of intervention. The dynamic effect of ice shedding on transmission lines has two major categories of concerns: electrical and mechanical. Lack of clearance between adjacent cables, cables and towers, and cables and the ground may lead to flashover or electrical shock. From the mechanical point of view, high-amplitude vibrations may cause the impact of suspension strings on towers, which may break the insulator; whereas the associated excessive tension generated in the cables may result in large unbalanced loads on towers, possibly leading to tower collapse. As these problems can pose a major threat to the operational safety of a grid system, the recognition of the nature of stresses in atmospheric ice which cause ice shedding is essential.

Many factors influence ice shedding and most of them emanate from weather changes. One can divide these factors into two categories: the loads which create stresses in atmospheric ice, and the factors which determine the constitutive behaviour of ice. The former category includes

wind loads (such as loads from galloping, Aeolian vibration and wake-induced oscillation), ice loads (gravity and ice mass inertia) and other loads such as impact from a flying object and ice shedding in adjacent cables. The latter category involves the atmospheric conditions during ice accumulation, air temperature during ice shedding, load rate, and ice behaviour in crack nucleation and propagation.

Galloping of suspended cables has been studied by many researchers [1, 2, 4, 6]. Irvine and Caughey (1974) developed a linear theory for free vibration of a uniformly suspended cable in which both in-plane and out-of-plane motions were considered. The results of this theory have been used by many researchers to model galloping behaviour. Yu *et al* (1993) developed a three-degree-of-freedom model to describe and predict different galloping behaviours of a single iced electrical transmission line. Ohkuma *et al* (1998) focused on the effects of wind turbulence on galloping, and tried to explore the galloping behaviour of a four-bundle overhead transmission line in gusty winds. Luongo and Piccardo (1998) derived a two-degree-of-freedom model to examine the aeroelastic behaviour of a flexible elastic suspended cable driven by the mean wind speed blowing perpendicularly to the plane of the cable. Abdel-Rohman and Spencer (2004) used the results of Luongo and Piccardo (1998) to study the along-wind and across-wind response motion of a suspended cable. They also investigated the effect of a vertical viscous damper at a certain location of the cable.

Only a few of the vast number of publications concerning galloping are mentioned in the above paragraph. To the best of our knowledge, however, none of them discusses in detail the stresses which develop in the ice accretion during the vibration. In this research work, an attempt was made to estimate these stresses and their variations with respect to load variations during galloping. The calculation of cable galloping motion, developed by Abdel-Rohman and Spencer (2004) and Luongo and Piccardo (1998), was applied to a cable covered with atmospheric ice. The results of this calculation are the displacements of each point along the cable in vertical and transverse directions, as well as the aerodynamic forces and other loads on the ice. These results are used in a new model constructed using the ABAQUS finite element software. This model provides an estimation of the stress level in different parts of atmospheric ice on the cable and its variation through a galloping cycle.

## II. CALCULATION OF LOADS IN GALLOPING

Galloping of power transmission lines is one of the most important phenomena inducing stresses in the accreted atmospheric ice. The significant deformation of the iced cable during this high-amplitude vibration induces stresses in the atmospheric ice. This deformation can be estimated by modeling the cable motion in galloping and obtaining the position of each point along the cable. Therefore, the equation of motion describing cable galloping will be considered. For a more accurate estimation, the following forces and stresses should be applied on atmospheric ice: aerodynamic forces, additional tension in cable due to vibration, ice mass inertia and torque due to cable spring back.

Owing to the complexity of this problem, we have to simplify some sophisticated aspects of natural conditions, as follows:

- Normally, ice shapes on power transmission lines are not exactly cylindrical and uniform; it is more symmetrical in the middle of the span than in other parts. Nevertheless, it is assumed that ice shape is cylindrical and uniform all along the cable. However, in the calculation of wind loads on the cable, the functions of wind force obtained from wind tunnel tests for asymmetrically iced cables are used.
- Movements and vibrations of towers during galloping are negligible.
- Wind velocity does not change during galloping and it is uniform all along the cable.

#### A. Equation of cable motion

The basic equations of motion of a suspended cable are the following [1,3,4]

$$\frac{\partial}{\partial s}[(T_0 + T_a) \frac{\partial(x + D_x)}{\partial s}] = m \frac{\partial^2 D_x}{\partial t^2} \quad (1)$$

$$\frac{\partial}{\partial s}[(T_0 + T_a) \frac{\partial(y + D_y)}{\partial s}] = -mg + m \frac{\partial^2 D_y}{\partial t^2} + c \frac{\partial D_y}{\partial t} + F_1(s, t) \quad (2)$$

$$\frac{\partial}{\partial s}[(T_0 + T_a) \frac{\partial D_z}{\partial s}] = m \frac{\partial^2 D_z}{\partial t^2} + c \frac{\partial D_z}{\partial t} + F_2(s, t) \quad (3)$$

in which  $s$  is the spatial coordinate along the curved length of the cable;  $t$  is the time;  $x$  is the coordinate along the cable span;  $y(s)$  is the cable static profile;  $D_x(s, t)$ ,  $D_y(s, t)$  and  $D_z(s, t)$  are, respectively, the displacement in the horizontal, vertical and transverse directions (Fig.1),  $m$  is the cable mass per unit length, including ice mass,  $c$  is the damping coefficient per unit length,  $T_0$  is the static tension;  $T_a$  is the additional dynamic tension in the cable;  $F_1(s, t)$ , and  $F_2(s, t)$  are, respectively, the external loading per unit length in the vertical and transverse directions.

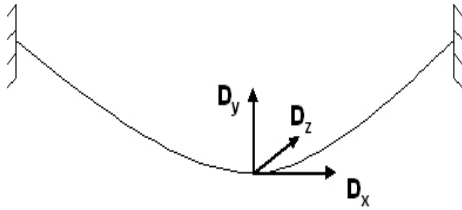


Fig 1. Cable displacement in horizontal,  $D_x$ , vertical,  $D_y$ , and transverse,  $D_z$ , directions

When additional dynamic tension is applied to the cable with accreted ice, this tension is divided between the cable and ice according to the following relations:

$$T_{ac} = T_a A_c E_c / (A_c E_c + A_i E_i) \quad (4)$$

$$T_{ai} = T_a A_i E_i / (A_c E_c + A_i E_i) \quad (5)$$

where  $E_i$  and  $E_c$  are Young's modulus of atmospheric ice and cable, and  $A_i$  and  $A_c$  are cross section areas of the ice and cable, respectively.

Since the ratio of sag to span in power transmission lines is less than 1:8 and horizontal loads are negligible in our model, we can consider the horizontal displacement  $D_x$  to be equal to zero [1,3]. The solution,  $D_y$  and  $D_z$ , of the equations of motion can be obtained by separation of variables:

$$D_y(s, t) = \varphi_1(s)W(t) \quad (6)$$

$$D_z(s, t) = \varphi_2(s)V(t) \quad (7)$$

where  $\varphi_1(s)$  and  $\varphi_2(s)$  are the mode shapes in the transverse and vertical directions respectively, and can be determined as [1]:

$$\varphi_1(s) = A_n \sin(n\pi s/l) \quad n=1, 2, 3, \dots \quad (8)$$

$$\varphi_2(s) = k_0 [1 - \tan(0.5\omega\pi) \sin(\pi\omega s/l) - \cos(\pi\omega s/l)] \quad (9)$$

where  $k_0$  is a constant chosen to make  $\varphi_2(l/2) = 1$ , and  $\omega = \omega_2 / \omega_1$ .  $\omega_1$  and  $\omega_2$ , the natural frequencies in the transverse and vertical directions, can be obtained as follows:

$$\omega_1 = n\pi\sqrt{H/m}/l \quad n=1, 2, 3, \dots \quad (10)$$

$$\omega_2 = q\sqrt{H/m} \quad (11)$$

with  $H$  denoting the horizontal component of cable tension which can be obtained by solving (12) numerically:

$$d = H[\cosh(mgl/2H) - 1]/mg \quad (12)$$

where  $d$  is the sag of the cable and  $q$  can be calculated from the following equation [3]:

$$\tan(ql/2) = (ql/2) - (4/\lambda^2)(ql/2)^3 \quad (13)$$

and where parameter  $\lambda^2$  takes the form:

$$\lambda^2 = (8d)^2 / (l(HL_e/E_c A_c)) \quad (14)$$

$$L_e = \int_0^l (ds/dx)^3 dx \approx l(1 + 8d^2/l^2) \quad (15)$$

In order to decrease the number of equations of motion and the complexity of analysis, this problem is solved for first mode shape only ( $n=1$ ). After simplifying (2) and (3), substituting (6) - (15) into them, and applying Galerkin's method, one obtains the equation of motion of the cable as follows [1]:

$$\ddot{W} + 2\xi_1\omega_1\dot{W} + \omega_1^2 W + n_5 W V^2 + n_6 W V^2 + n_7 W V^3 = F_1(t) \quad (16)$$

$$\ddot{V} + 2\xi_2\omega_2\dot{V} + \omega_2^2 V + n_1 V^2 + n_2 W^2 + n_3 V^3 + n_4 W V^2 + F_2(t) = 0 \quad (17)$$

where  $\xi_1$  and  $\xi_2$  are damping ratios in transverse and vertical directions, whereas  $F_1(t)$  and  $F_2(t)$  are determined as below

$$F_1(t) = d_0 + d_1\dot{W} + d_2\dot{W}^2 + d_3\dot{V} + d_4\dot{W}\dot{V} + d_5\dot{V}^2 + \sum_{k=3}^N d_{(2k)}\dot{V}^k + \sum_{k=3}^N d_{(2k+1)}\dot{V}^k\dot{W}^{(k-2)} \quad (18)$$

$$F_2(t) = e_0 + e_1\dot{W} + e_2\dot{W}^2 + e_3\dot{V} + e_4\dot{W}\dot{V} + e_5\dot{V}^2 + \sum_{k=3}^N e_{(2k)}\dot{V}^k + \sum_{k=3}^N e_{(2k+1)}\dot{V}^k\dot{W}^{(k-2)} \quad (19)$$

The coefficients  $n_i$ ,  $d_i$  and  $e_i$  are defined in Kermani (2006).

Finally, the equations of motion of a galloping cable can be written by combining (16) and (17) with (18) and (19), yielding:

$$\ddot{W} + 2\xi_1\omega_1\dot{W} + \omega_1^2W + n_3WV^2 + n_6WV^2 + n_7WV^3 = d_0 + d_1\dot{W} + d_2\dot{W}^2 + d_3\dot{V} + d_4\dot{W}\dot{V} + d_5\dot{V}^2 + \sum_{k=3}^N d_{(2k)}\dot{V}^k + \sum_{k=3}^N d_{(2k+1)}\dot{V}^k\dot{W}^{(k-2)} \quad (20)$$

$$\ddot{V} + 2\xi_2\omega_2\dot{V} + \omega_2^2V + n_1V^2 + n_2W^2 + n_3V^3 + n_4WV^2 + e_0 + e_1\dot{W} + e_2\dot{W}^2 + e_3\dot{V} + e_4\dot{W}\dot{V} + e_5\dot{V}^2 + \sum_{k=3}^N e_{(2k)}\dot{V}^k + \sum_{k=3}^N e_{(2k+1)}\dot{V}^k\dot{W}^{(k-2)} = 0 \quad (21)$$

### B. Loads and stresses in atmospheric ice due to cable bending

The most important type of stress involved in ice shedding from power transmission lines during galloping is the bending stress. When galloping causes the cable to bend, the atmospheric ice on the cable resists against this deformation. However, if the force overcomes the resistance of the atmospheric ice, the ice breaks and may shed. The position of each point along the cable during galloping (results of the calculations presented in Section 2.1) will be used in the ABAQUS model to determine the stresses developing in atmospheric ice.

#### • Aerodynamic forces

As mentioned above, aerodynamic forces cause cable galloping, and the ensuing movement can produce bending moment and additional tension in the cable. However, these forces apply some loads directly on the accreted ice too. Equations (18) and (19) express the loads of the aerodynamic force per unit length in the transverse and vertical directions, respectively. To take into account the effect of these forces on a piece of atmospheric ice in the middle of a span, it is sufficient to apply them in the ABAQUS model as a distributed force on the ice (see Fig. 2).

#### • Torsional loads

Power transmission cables are very flexible and tend to rotate when ice builds up asymmetrically on their surface. Due to such a rotation, the ice mass tends to be evenly distributed on the surface of the cable. This can explain why the ice shape observed on transmission lines is predominantly circular. During ice accretion, when the ice on the cable is not symmetric, two factors can apply torsional load on the cable, ice weight and aerodynamic force due to wind speed. However, when ice accumulates on the cable and takes a cylindrical shape, the torsional load due to wind becomes negligible. The rotational angle of the iced cable depends upon the torsional rigidity of the cable and the amount of ice accreted on it.

The relationship between the rotation of the cable at mid-span around its centerline,  $\theta$ , and the torque at the suspension points,  $T_A$ , due to cable spring back can be written as follows :

$$T_A L / 2GJ = \theta \quad (22)$$

where  $GJ$  is torsional rigidity of cable,  $L$  is cable length, and constant ice thickness is assumed along the entire span. Once  $\theta$  is known, the spring-back torque  $T_C$ , which is applied by

the cable to the end point of a piece of ice located in the middle of the span, can be determined as follows:

$$T_C = 2\theta L_1 GJ / L^2 \quad (23)$$

where  $L_1$  is the length of piece of cable (torque in Fig. 2). Since a short piece of the cable-ice composition in the middle of the span is analyzed, i.e.  $L_1 \ll L$ , the torque,  $T_C$ , is significantly smaller than the other loads discussed above.

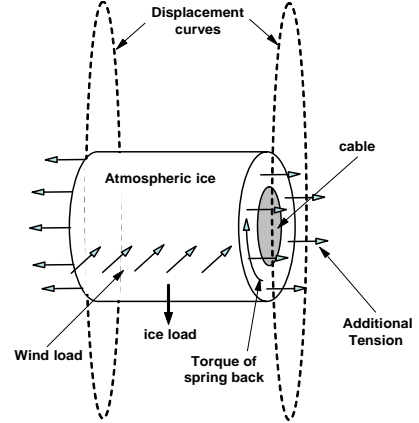


Fig 2. Loads and movement of a piece of cable on corresponding curves

#### • Additional tension in the cable and the ice

As mentioned above, cable motion during galloping induces additional tension in the cable and the atmospheric ice. The stresses due to these additional tensions are calculated using the following formulae:

$$\sigma_c = E_c(ds' - ds) / ds \quad (24)$$

$$\sigma_i = E_i(ds' - ds) / ds \quad (25)$$

where  $ds'$  is the deformed cable segment. These terms were considered in the model developed in ABAQUS (additional tensions in Fig. 2).

#### • Load due to ice mass inertia

The ice load is induced by acceleration due to cable motion or gravity force. In this model the effect of this load is calculated using the ABAQUS software.

### C. Calculation of forces and displacements

In order to obtain the displacement of each point of cable during galloping (as mentioned in Section 2.1), the constants  $n_i$ ,  $d_i$ , and  $e_i$  in (20) and (21) should be determined first. These constants together with the initial cable tension,  $T_0$ , and the natural frequencies in transverse and vertical directions,  $\omega_1$  and  $\omega_2$ , are calculated by a code written in MAPLE. The output data of this code are scalars corresponding to  $T_0$ ,  $\omega_1$  and  $\omega_2$ , as well as three matrices providing the constants  $n_i$  ( $1 \times 7$ ),  $d_i$  ( $1 \times 15$ ) and  $e_i$  ( $1 \times 15$ ).

The cable motion during galloping is simulated by a program developed in MATLAB. All the results provided by the MAPLE code, the cable and ice characteristics, the wind velocity,  $U_0$ , and the damping ratios in the vertical and transverse directions,  $\xi_1$  and  $\xi_2$  are defined as input data for

the MATLAB implementation. This program solves (20) and (21) numerically and determines the displacement of the two ends of a length of cable with ice in the middle of the span. Furthermore, it computes the aerodynamic forces on the ice, the torque applied to the ice due to cable spring back, and the additional tension in the cable and the ice. All of these values are tabulated as time functions, and then are used as loads and displacement in the ABAQUS model described in the next section.

### III. MODELING STRESS VARIATION DURING GALLOPING

The simulation of cable motion and the load calculation provide all the parameters needed to determine the stress in the ice and its variation during galloping. A model consisting of a length of cable with uniform cylindrical ice accretion is designed with ABAQUS, which then computes the stress developing in the ice through one or more cycles of galloping. The curves representing cable motion at each end of the modeled piece, as sketched in Fig. 2, are obtained as output data of the MATLAB program. The additional cable tension and aerodynamic forces are also added as input data, while the effect of ice load and inertia is calculated by ABAQUS. Fig. 2 shows schematically the movement of a piece of cable, as well as the forces and the torque applied on the accreted ice.

The analysis was carried out in the Dynamic Explicit condition mode with ABAQUS, which uses a consistent, large-deformation theory and where the model can undergo large rotations and large deformation. The element type for cable and ice is C3D8R. This is a three-dimensional element with 8 nodes and suitable for continuum stress/displacement analysis with reduced integration. The variations of transverse and vertical displacements, aerodynamic forces, additional tension in the cable and the ice were tabulated in 8 tables. Each table has two columns, the first one containing the time data, and the other one listing the above-mentioned parameters at each instance. The total time of analysis is 3.33 s. In order to have more accurate estimation, both ends of the cable-ice piece at the beginning of the analysis were set in the positions which represent the initial shape of the ice and cable before any deformation. The ice was assumed to adhere strongly to the cable surface without sliding and separation.

### IV. RESULTS AND DISCUSSION

The preliminary calculations with MAPLE, the galloping simulation with MATLAB and the stress analysis in ABAQUS were applied to a typical example. Table 1 shows the characteristics of the span, cable and ice considered in this example.

Preliminary calculations were first carried out with the data presented in Table 1, and then the galloping of the cable-ice composition was simulated. The cable displacement at mid-span in the transverse and vertical directions is shown in Fig. 3. A full cycle of galloping lasts 3.33 s, and it is clear that the amplitude of the vertical motion is significantly greater than that of the transverse motion. The trajectory of the mid-point of the cable is shown in Fig. 4. The results of wind load and stress calculations are presented in Figs. 5 and 6. Fig. 5 shows the variations of distributed wind forces in vertical and

transverse directions during a full cycle of vibration, whereas Fig. 6 shows the stresses due to additional tension in the cable and accreted ice.

Table1. Characteristics of the span, cable and ice

Parameter	Value	Unit
Cable type	BERSIMIS ACSR 42/7	---
Cable diameter	35.1	mm
Young's modulus of cable	62	GPa
Mass per unit length of cable	2.185	kg/m
Cable torsional rigidity	351	N.m/Rad
Cable cross-section area	725.2	mm <sup>2</sup>
Span length	300	m
Cable sag	8.04	m
Ice type	Hard rime and glaze	---
Ice thickness on cable	25	mm
Density of ice	900	Kg/m <sup>3</sup>
Young's modulus of ice	9	GPa
Wind velocity	6	m/s
Rotation angle due to ice	405°	Degree

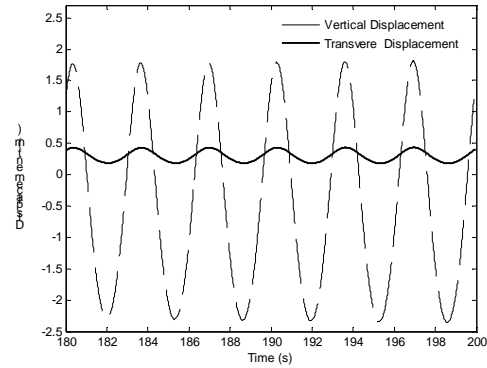


Fig. 3. Cable displacement at mid-span during galloping.

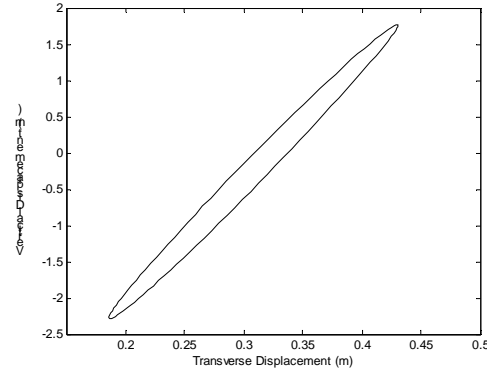


Fig. 4. The trajectory of mid-point of cable during galloping.

#### A. Galloping simulation

The data presented in Table 1 and the results of calculations discussed in Section 4.1 were applied as input for the stress analysis on a piece of cable-ice composition in the middle of the span. The length of this piece was set at 10 cm.

Stresses in several elements modeling the ice were calculated during one cycle of galloping and the results for elements in various positions are shown in Figs. 7 and 8. Fig. 9 illustrates the positions of these elements in the middle of the 10-cm piece of ice cover. As shown in Figs. 8 and 9, the Von Mises stresses reach their maximum values at 1.27 s and 2.9 s, when the mid-point of the cable is at the highest and lowest position of its trajectory, respectively. Numerically, these maximum values are 7.33 MPa and 5.61 MPa for the elements in the external layer, and 4.99 MPa and 3.59 MPa for

the element in the internal layer. According to Fig. 4, the vertical displacement of the cable reaches its limits twice in one cycle: first at 1.27 s when the mid-point of the cable is at the highest position of its trajectory, and then at 2.9 s when this point reaches the lowest position. The stress is greater in the first case, because the transverse position of the mid-point of the cable is the farthest from its location in static equilibrium at 1.27 s, while it is the nearest at 2.9 s.

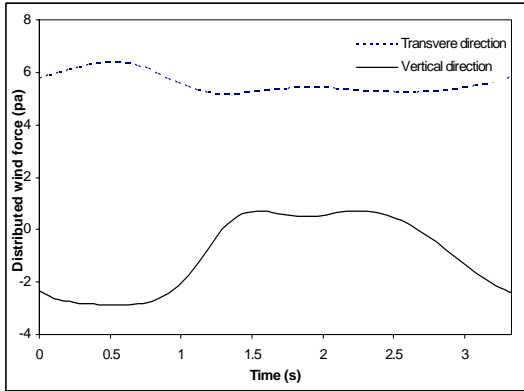


Fig. 5. Variations of distributed wind force in transverse and vertical directions.

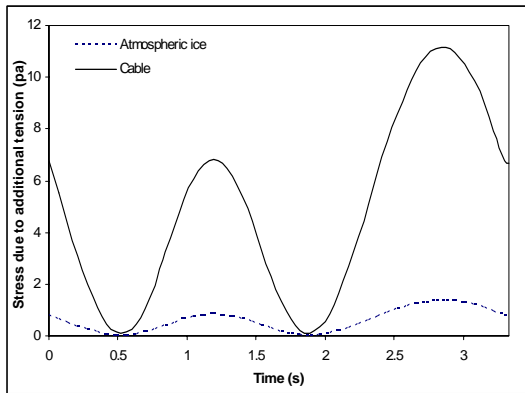


Fig. 6. Variations of stresses due to additional tension in cable.

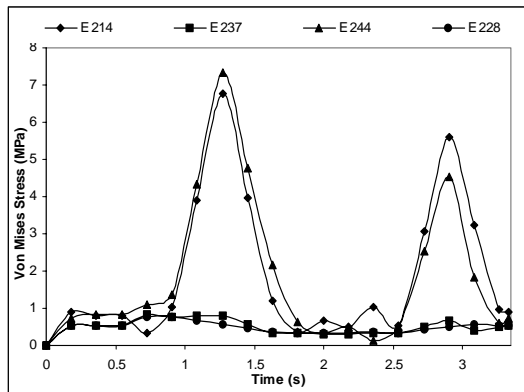


Fig 7. Stresses in 4 elements in the external layer of atmospheric ice.

### B. Stress analysis

The mechanical properties of atmospheric ice under mechanical stress were examined in a parallel research, the results of which will be published later [5]. According to those observations, the bending strength of atmospheric ice at  $-10\text{ }^{\circ}\text{C}$  varies with strain rate, but it may be approximately assumed to be 3.4 MPa. Although the von Mises stress is not equivalent to the bending stress, it mainly arises from the bending load in

our case. Thus, since the von Mises stress is significantly greater for some ice elements than the bending strength of ice, our model predicts ice fracture from the part of the cable under examination. Ice failure is initiated at the top and bottom sides of the accreted ice sheath, because stresses are higher at these locations, whereas stress level does not exceed the bending strength for the lateral elements on the left and right sides of the cable. A section of iced cable with stress distribution is illustrated in Fig.10.

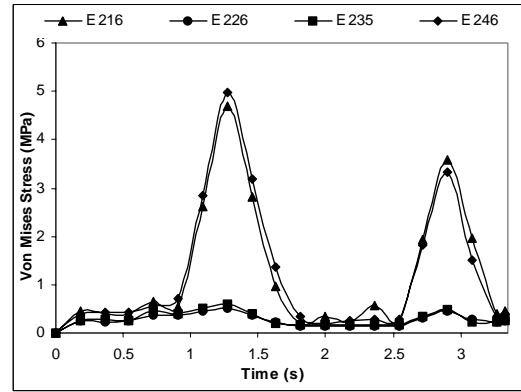


Fig 8. Stresses in 4 elements in the internal layer of accreted ice.

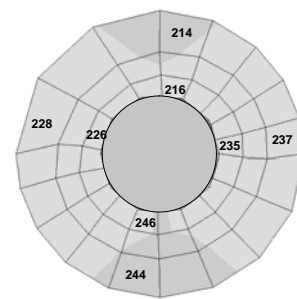


Fig 9. Position of elements which are the objects of Figs. 8, 9, 12 and 13.

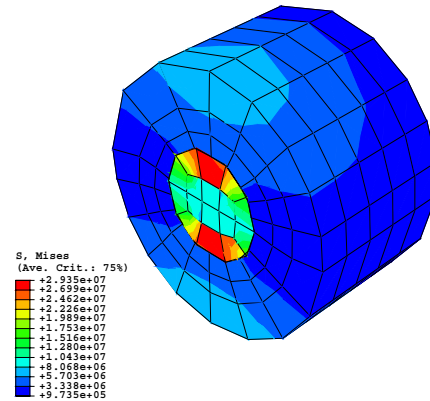


Fig. 10. Stress distribution in cable and accreted ice.

Figs. 11 and 12 show normal stresses parallel to cable axis for the same elements as in Figs. 7 and 8, respectively. When the cable approaches its highest position, the elements on the top of the cable (elements No. 214 and 216) will be under tension, whereas the bottom elements (No. 244 and 246) will be under compression. The direction of stresses changes when the cable approaches its lowest position. The elements which are on the neutral axis (elements No. 228, 226, 235 and 237) bear the minimum normal stress arising from the additional horizontal tension caused by the cable motion. Figs. 13 and 14 show the distribution of Von Mises stress along the horizontal

and vertical diameters of the iced cable in the middle of the 10-cm piece. As expected, stress in the internal layers of the ice (and cable) is less than that of the external layers.

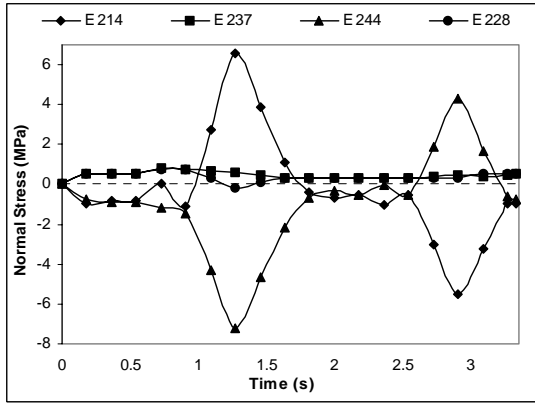


Fig 11. Normal stresses in 4 elements in the external layer of accreted ice.

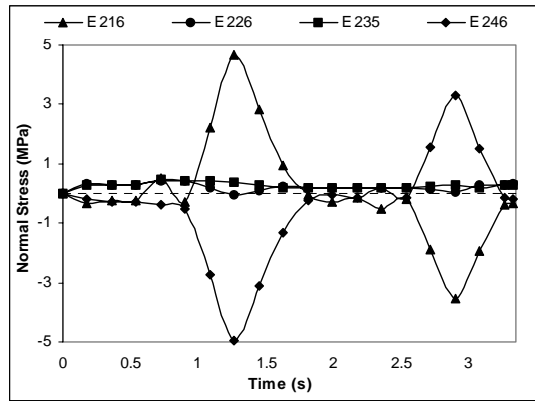


Fig 12. Normal stresses in 4 elements in the internal layer of accreted ice.

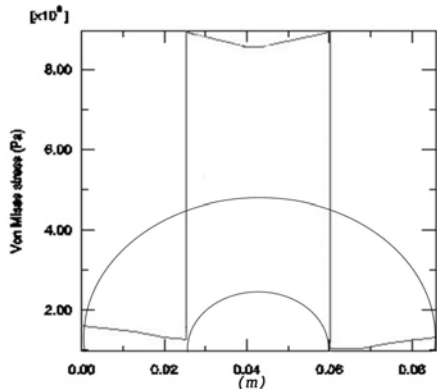


Fig13. Stress distribution along horizontal diameter of cable-ice composition.

## V. CONCLUSION

This paper presents a finite element model for estimating galloping induces stress in the ice cover of an overhead cable. In order to determine the displacement and load data which serve as input for this model, galloping of an iced cable was simulated. Equations of cable motion, derived for galloping in former publications, were applied to an iced cable, and solved by a MATLAB code to obtain time histories of cable motion, aerodynamic forces, additional horizontal tension acting in the cable during vibration and torque due to spring back. For this purpose, a 10-cm-long piece of iced cable at mid-span was

considered, the input data being determined at the two end points of the piece. The finite element model was constructed using the ABAQUS commercial software for calculating the stresses in the atmospheric ice accreted on the cable. The model revealed that the higher stresses occurred along the vertical diameter of the ice when the mid-point of the cable reached the highest or lowest positions of its trajectory. As these stresses exceeded the bending strength of ice in the particular case at hand, the model predicted ice failure. Using the method and model proposed in this investigation, the level of stress in atmospheric ice may be estimated for any other loading condition.

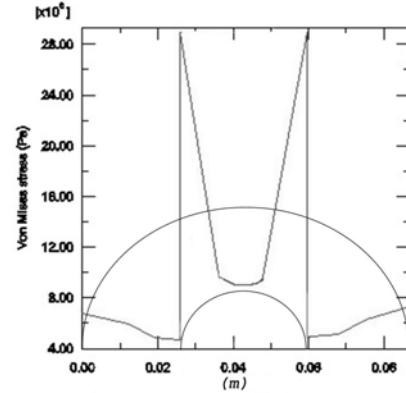


Fig14. Stress distribution along vertical diameter of cable-ice composition.

## VI. ACKNOWLEDGEMENTS

This work was carried out within the framework of the NSERC/Hydro-Quebec/UQAC Industrial Chair on Atmospheric Icing of Power Network Equipment (CIGELE) and the Canada Research Chair on Engineering of Power Network Atmospheric Icing (INGIVRE) at Université du Québec à Chicoutimi. The authors would like to thank the CIGELE partners (Hydro-Québec, Hydro One, Électricité de France, Alcan Cable, K-Line Insulators, CQRDA and FUQAC) whose financial support made this research possible.

## VII. REFERENCES

- [1] Abdel-Rohman, M., and Spencer, B. F. (2004). "Control of Wind-Induced Nonlinear Oscillations in Suspended Cables." *Nonlinear Dynamics*, 37, 341-355.
- [2] Yu, P., Desai, Y. M., Shah, A. H., Popplewell, N. (1993). "Three-degree-of-freedom model for galloping. Part II: Solutions." *Journal of Engineering Mechanics*, 119(12), 2426-2448.
- [3] Irvine, H. M., and Caughey, T. K. (1974). "The linear theory of free vibration of a suspended cable." *Proc. R. Soc. Lond. A*, 341, 299-315.
- [4] Luongo, A., and Piccardo, G. (1998). "Non-linear galloping of sagged cables in 1:2 internal resonance." *Journal of Sound and Vibration*, 214(5), 915-940.
- [5] Kermani, M. (2007). *Ice shedding from cables and conductors - a model of cracking activity of atmospheric ice in brittle regime*, Ph.D. thesis, University of Quebec at Chicoutimi, QC, Canada, to be submitted.
- [6] Ohkuma, T., Kagami J., Nakauchi H., Kikuchi T., Takeda K., Marukawa H. (2000). "Numerical Analysis of Overhead Transmission Line Galloping Considering Wind Turbulence." *Electrical Engineering in Japan*, 131(3), 1386-1397.